Dielectric Properties of Relaxor-like Vinylidene Fluoride−Trifluoroethylene-Based Electroactive Polymers

V. Bobnar,* B. Vodopivec, and A. Levstik

Condensed Matter Physics Department, Jožef Stefan Institute, P.O. Box 3000, SI-1001 Ljubljana, Slovenia

M. Kosec

Electronic Ceramics Department, Jožef Stefan Institute, P.O. Box 3000, SI-1001 Ljubljana, Slovenia

B. Hilczer

Institute of Molecular Physics, Polish Academy of Sciences, PL-60179 Poznan, Poland

Q. M. Zhang

Materials Research Institute, The Pennsylvania State University, University Park, Pennsylvania 16802

Received February 5, 2003; Revised Manuscript Received April 1, 2003

ABSTRACT: The dynamic processes in poly(vinylidene fluoride−trifluoroethylene) (P(VDF−TrFE)) copolymer, lead lanthanum zirconate titanate (PLZT)−P(VDF−TrFE) composite, electron-irradiated P(VDF−TrFE) copolymer, and poly(vinylidene fluoride−trifluoroethylene−chlorofluoroethylene) (P(VDF−TrFE−CFE)) terpolymer have been studied by measurements of the temperature and frequency-dependent linear (ϵ_1) and third-order nonlinear (ϵ_3) dielectric constants. While a paraelectric-to-ferroelectric transition takes place in the crystalline region of the nonirradiated copolymer and composite, electron-irradiated P(VDF−TrFE) copolymer and P(VDF−TrFE−CFE) terpolymer show a significantly different dielectric response: a broad frequency dispersion in ϵ_1 and ϵ_3, asymmetric temperature evolution of the relaxation spectrum as the longest relaxation time diverges at a finite freezing temperature while the shortest relaxation times remain active down to the lowest temperatures, and a paraelectric-to-glass crossover in the temperature dependence of the dielectric nonlinearity $a_3 = \epsilon_3/\epsilon_0^3\epsilon_1^4$. All these properties, together with the temperature dependence of the static field cooled dielectric constant, are very similar to those observed in the classical relaxor systems and are reminiscent of the dynamic behavior observed in various spin glasses. Thus, additional confirmation that giant electrostrictive response of the electron-irradiated P(VDF−TrFE) copolymer and P(VDF−TrFE−CFE) terpolymer is the consequence of their relaxor-like structure is obtained.

I. Introduction

Ever since the high piezoelectric effect in poly(vinylidene fluoride) (PVDF) has been reported,[1] these polymers have played an important role in sensor and actuator applications. Similarly, the high piezoelectric effect has been found in poly(vinylidene fluoride−trifluoroethylene), P(VDF−TrFE), copolymer. Contrary to PVDF, this system spontaneously crystallizes into the polar phase, and discovery of ferroelectricity in such an organic compound clearly attracted a great interest.[2−6] Just recently, dielectric properties of lead lanthanum zirconate titanate (PLZT)−P(VDF−TrFE) composite have been reported.[7] As in P(VDF−TrFE) copolymer, a paraelectric-to-ferroelectric phase transition takes place in the crystalline region of this composite. However, the PLZT−P(VDF−TrFE) composite might present an example of a piezoactive system whose dielectric properties can be relatively easy tuned. The fact that it can also be easily prepared in a variety of shapes makes it a very promising material for numerous applications.

Further manipulation of the P(VDF−TrFE) copolymer resulted in materials with additional exciting physical properties. For example, a polymorphic transformation of the ferroelectric phase to a paraelectric-like structure, induced by γ-rays[8] or high-energy electron irradiation,[9] has been observed in P(VDF−TrFE) copolymer. Recently, a giant electrostrictive response of electron-irradiated P(VDF−TrFE) copolymer,[10] poly(vinylidene fluoride−trifluoroethylene−chlorotrifluoroethylene), P(VDF−TrFE−CTFE), terpolymer,[11] and poly(vinylidene fluoride−trifluoroethylene−chlorofluoroethylene), P(VDF−TrFE−CFE), terpolymer,[12] has been reported. It was suggested that an ultrahigh strain response in all three systems is generated due to expanding of the polar regions under external electric field, coupled with a large difference in the lattice strain between polar and nonpolar phases. Namely, these systems exhibit typical relaxor behavior, suggesting that irradiation with high-energy electrons or introduction of CFE (CTFE) converts coherent polarization domain (all-trans chains) in normal ferroelectric P(VDF−TrFE) copolymer into nanopolar regions, thus transforming the material into a relaxor ferroelectric system.

Classical relaxor systems, such as lead magnesium niobate (PMN) and PLZT ceramics, are characterized by a broad frequency dispersion in the complex dielectric constant, slowing dynamics, and logarithmic polarization decay.[13] These systems are believed to provide a conceptual link between ferroelectrics and dipolar glasses. Namely, in zero electric field no long-range ferroelectric

* Corresponding author: e-mail vid.bobnar@ijs.si.

10.1021/ma034149h CCC: $25.00
Published on Web 05/23/2003

state is established, and relaxors undergo a freezing transition into the nonergodic state.[13] On the other hand, by cooling the relaxor material in an electric field higher than the critical field, a long-range ferroelectric phase is formed.[14]

Intensive investigations of electron-irradiated P(VDF−TrFE) copolymer, carried out in the recent years,[15−18] indeed revealed some typical relaxor properties, like broad dispersive dielectric maximum and slowing down of the characteristic relaxation time according to the Vogel−Fulcher law.[18] To deepen our knowledge of relaxor-like properties of VDF−TrFE-based electroactive polymers, dielectric dynamics in electron-irradiated P(VDF−TrFE) copolymer and P(VDF−TrFE−CFE) terpolymer has been studied by a detailed measurements of the temperature and frequency-dependent linear and third-order nonlinear complex dielectric constants. Analysis of the linear dielectric response by a temperature−frequency plot has revealed that, like in various spin glasses and classical relaxors,[19,20] the ergodicity is broken at the freezing transition temperature T_f due to the divergence of the longest relaxation time, while the bulk of the relaxation spectrum remains finite below T_f. Also, the temperature dependences of the static field-cooled dielectric constant and dielectric nonlinearity $a_3 = \epsilon_3/\epsilon_0^3\,\epsilon_1^4$, where ϵ_1 and ϵ_3 are linear and third-order nonlinear dielectric constants, respectively, were found to be very similar to that observed in the classical relaxor systems. Especially a_3 turned out to be a powerful tool for investigations of relaxor properties: its temperature dependence can in fact distinguish between ferroelectric and glass transitions, as a_3 should vanish at ferroelectric or diverge at glass transition.[21]

A relaxor-like dielectric response of P(VDF−TrFE−CFE) terpolymer is particularly emphasized in the paper. This recently developed system has several advantages over electron-irradiated P(VDF−TrFE) copolymer, which also shows giant electrostrictive response. Namely, elimination of the irradiation process simplifies the processing and also removes the undesirable side effects of irradiation, such as formation of radicals, chain scission, and cross-linking.

II. Experimental Procedures

A. Materials Preparation. P(VDF−TrFE) copolymer samples with a VDF content of 50 mol % (50/50 samples) were obtained from the copolymer powder by hot pressing at T = 450 K and p = 600 MPa for 30 min. The same parameters were used for hot pressing of $(Pb_{0.905}La_{0.095})(Zr_{0.65}Ti_{0.35})O_3$ relaxor ceramic and P(VDF−TrFE) 50/50 ferroelectric copolymer powders in order to obtain PLZT−P(VDF−TrFE) composite. PLZT powder was prepared using PbO, lanthanum acetate aqueous solution, and zirconium and titanium alkoxide solutions.[22] Copolymer samples with the thickness of 55 μm and composite samples with 0.24 ceramic volumetric fraction and thickness of 120 μm were covered with sputtered gold electrodes having a diameter of 11 mm.

P(VDF−TrFE−CFE) terpolymer films with a thickness of 15 μm were prepared using the solution-cast method by first dissolving P(VDF−TrFE−CFE), synthesized by a suspension polymerization process, in dimethylformamide. The composition of investigated films was 68/32/9, where 68/32 is the mole ratio of VDF/TrFE and 9 is the mole ratio of CFE in the terpolymer. The VDF/TrFE ratio was evaluated from the ^{19}F NMR spectrum, while the CFE mol % was determined by element analysis. The films were subsequently annealed at $T \approx 120$ °C for 6 h in order to improve their crystallinity. Similarly, 10 μm thick P(VDF−TrFE) 55/45 copolymer films were prepared for the irradiation process. The electron irradiation was carried out in a nitrogen atmosphere at 373 K with 1.2 MeV electrons. While earlier investigations were carried out in copolymers irradiated with electrons of higher energies,[10,15,17,18] it was found out recently that irradiation at a temperature above a paraelectric-to-ferroelectric transition reduces the electrons energy and the irradiation dose, needed to achieve high electrostrictive response.[23] An irradiation dose of 55 Mrad was chosen, thus being in the range 40−100 Mrad, where the irradiated copolymer exhibits relaxor behavior.[18,23] Silver paste electrodes were used for dielectric measurements of both relaxor-like systems.

B. Dielectric Measurements. Complex linear dielectric constant $\epsilon_1^*(\omega,T) = \epsilon_1' - i\epsilon_1''$ was measured in the frequency range 20 Hz−1 MHz by using a HP 4284A Precision LCR meter. The amplitude of the probing ac electric signal was 1 V. After heating the samples to 350−375 K, the dielectric response was detected during cooling and subsequent heating runs with the rate of ±0.5 K/min. A similar heating/cooling procedure was used for the third-order nonlinear dielectric response measurements, which were carried out at several frequencies between 1 Hz and 10 kHz by using a HP35665A dynamic signal analyzer. Here, the first, ϵ_1, and the third, ϵ_3, harmonic dielectric responses were measured simultaneously, which, in comparison to the separate measurement runs, reduces mistake in the subsequent computation of the ratio $a_3 = \epsilon_3/\epsilon_0^3\,\epsilon_1^4$. In this computation, real parts of the linear and third-order nonlinear dielectric constant were used.

The temperature dependence of the static dielectric constant can be measured by using the corresponding method described in ref 24. The external electric field E is applied at the highest temperature in the desired temperature measurement range. Then, during cooling the sample in electric field the corresponding polarization P_{FC} (FC denotes field cooled) is monitored via charge accumulation technique using a Keithley 617 programmable electrometer. The static dielectric constant ϵ_s can be calculated directly from the dielectric polarization as $\epsilon_s = 1 + P_{FC}(E,T)/\epsilon_0 E$. In our case, relatively high electrical conductivity of polymers prevents charge measurements at temperatures above 300 K; therefore, a slightly modified method was adopted. Samples were first cooled in zero electric field to a fixed temperature, where the conductivity was sufficiently low, and then the external electric field was applied. After the measured charge reached its saturated value ($P_{FC} = P_{ZFC}(t \to \infty)$), the static dielectric polarization, i.e., static dielectric constant, was measured during subsequent cooling of the sample.

The temperature of the samples was stabilized within ±0.01 K by using a lock-in bridge technique with a platinum resistor Pt100 as a thermometer.

III. Results and Analysis

This section gives a description of the linear and nonlinear dielectric response of the ferroelectric P(VDF−TrFE) copolymer and PLZT−P(VDF−TrFE) composite, as well as of the relaxor-like P(VDF−TrFE−CFE) terpolymer and electron-irradiated P(VDF−TrFE) copolymer.

A. Dielectric Properties of P(VDF−TrFE) Copolymer and PLZT−P(VDF−TrFE) Composite. Figure 1 shows the temperature dependence of the real, ϵ_1', and imaginary, ϵ_1'', parts of the complex linear dielectric constant, measured at several different frequencies in P(VDF−TrFE) copolymer. The most distinctive feature is a peak in both ϵ_1' and ϵ_1'' at $T_c \approx 343$ K, which denotes the phase transition from the distorted trans−gauche paraelectric to all-trans ferroelectric phase, occurring in the crystalline region of the copolymer.[2,4,17,25] Although it has been shown by ac calorimetric studies that by decreasing the VDF content in copolymer the nature of this phase transition changes from the first to the second order,[26] a small thermal

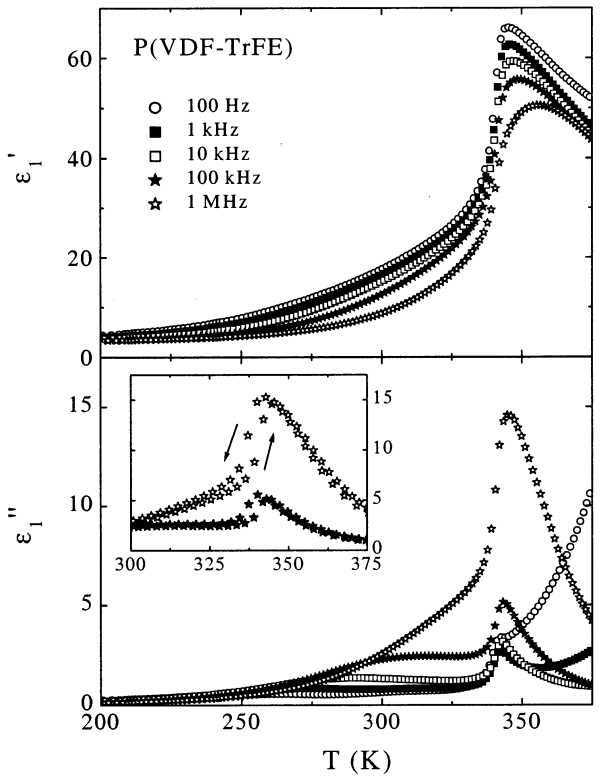

Figure 1. Temperature dependence of the real, ϵ_1', and imaginary, ϵ_1'', parts of the complex linear dielectric constant, measured at several different frequencies in the P(VDF−TrFE) copolymer. The inset shows thermal hysteresis detected during cooling/heating runs.

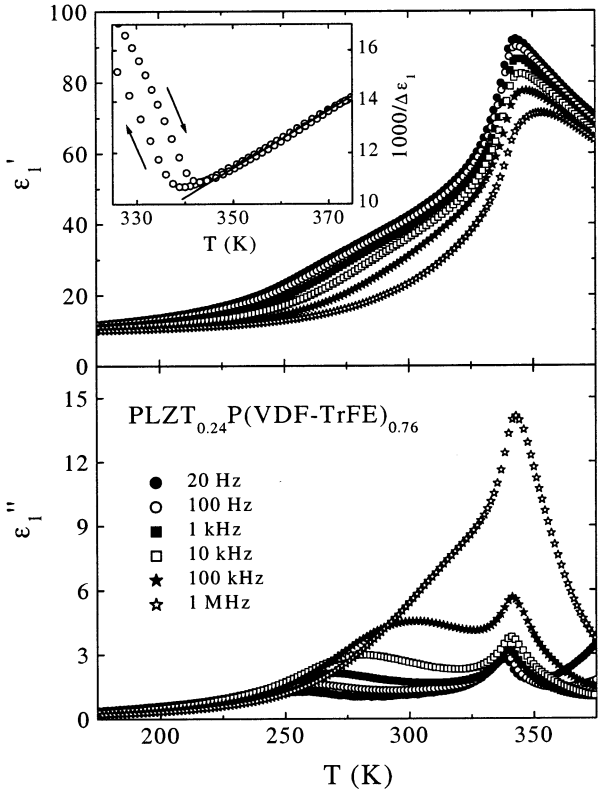

Figure 2. Temperature dependence of the real, ϵ_1', and imaginary, ϵ_1'', parts of the complex linear dielectric constant, measured at several different frequencies in the PLZT−P(VDF−TrFE) composite. The inset shows thermal hysteresis detected during cooling/heating runs and Curie−Weiss behavior above T_c.

hysteresis during cooling and subsequent heating run can still be observed, as is shown in the inset to Figure 1.

The second feature in the dielectric spectra of P(VDF−TrFE) copolymer, presented in Figure 1, is a dielectric relaxation in the temperature region of 275−335 K. This so-called β-process is without ambiguity associated with the dynamic manifestation of the glass transition in the amorphous phase of copolymer, i.e., a transition from the glassy to rubbery state.[4,17,25] Earlier studies have shown that the temperature dependence of the characteristic relaxation time of β-relaxation is of WLF-type (Williams, Landel, and Ferry), thus being clearly different than the Arrhenius-type relaxation process, which also occurs at low temperatures in the crystalline region of copolymer.[17]

Figure 2 shows the temperature dependence of the real and imaginary parts of the complex linear dielectric constant, measured at several different frequencies in the PLZT−P(VDF−TrFE) composite. As in the P(VDF−TrFE) copolymer, the paraelectric-to-ferroelectric phase transition and β-relaxation were detected. The inset to Figure 2 shows thermal hysteresis detected during cooling and subsequent heating runs and typical Curie−Weiss behavior of the dielectric strength $\Delta\epsilon_1 = \epsilon_s - \epsilon_\infty \propto 1/(T - T_c)$. Here, the static dielectric constant ϵ_s was identified with ϵ_1' measured at the frequency of 20 Hz, while the value of $\epsilon_\infty = 9$, which is the dielectric constant at high frequencies and takes into account the ionic and electronic polarizability of the system, and is in copolymer usually almost independent of the temperature, was determined from ϵ_1' data measured at 1 MHz at the lowest temperatures.

The dielectric response of the PLZT−P(VDF−TrFE) composite is therefore very similar to that observed in the P(VDF−TrFE) copolymer. Although ϵ_1' and ϵ_1'' values in composite are due to the high values of the dielectric constant of PLZT ceramics higher than those in copolymer, the dielectric relaxation processes of the ferroelectric copolymer obviously determine the dielectric response of the composite. Increase in dielectric constant due to the PLZT admixture suggests that this composite might present an example of a piezoactive system whose dielectric properties could be relatively easy tuned by changing the PLZT/copolymer ratio.

Figure 3 shows the temperature dependences of the third-order nonlinear dielectric constant ϵ_3 and dielectric nonlinearity $a_3 = \epsilon_3/\epsilon_0{}^3\epsilon_1{}^4$, measured at three different frequencies. The inset to Figure 3 shows decreasing of a_3 when approaching the paraelectric-to-ferroelectric phase transition. The scaling theory in fact predicts that a_3 should vanish at the paraelectric-to-ferroelectric phase transition.[27] However, at T_c a distinctive change of $a_3(T)$ slope occurs, and below T_c a_3 increases with further decreasing of the temperature. This is most probably the consequence of the glass transition in the amorphous phase, as a_3 should diverge at the freezing transition in dipolar glasses.[28] Of course, the scaling theory predicts behavior of the static quantities, while here dynamic results are presented. However, at temperatures around the paraelectric-to-ferroelectric phase transition, where there is almost no frequency dispersion in a_3, i.e., the dynamic results can be identified with the static quantites, its temperature dependence follows theoretical predictions. At lower temperatures, below

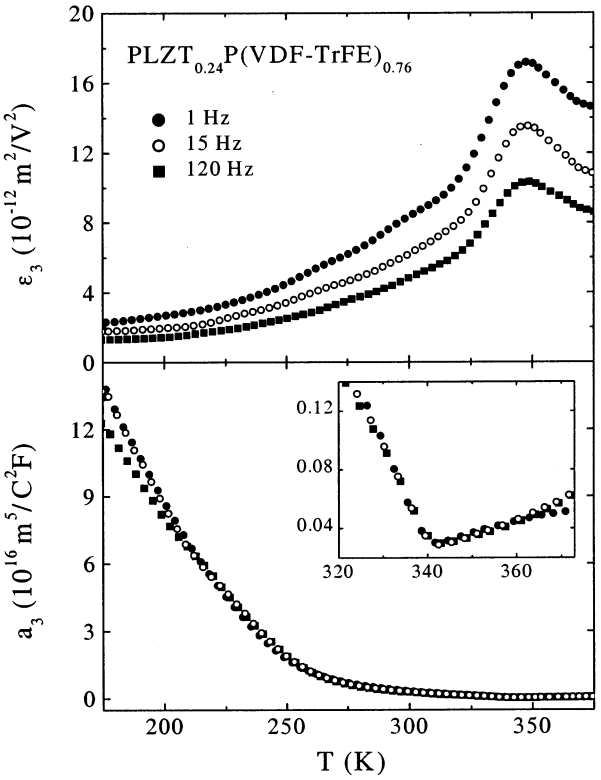

Figure 3. Temperature dependences of the third-order nonlinear dielectric constant ϵ_3 and dielectric nonlinearity a_3, measured at three different frequencies in the PLZT−P(VDF−TrFE) composite. The inset shows a_3 in the vicinity of the paraelectric-to-ferroelectric phase transition.

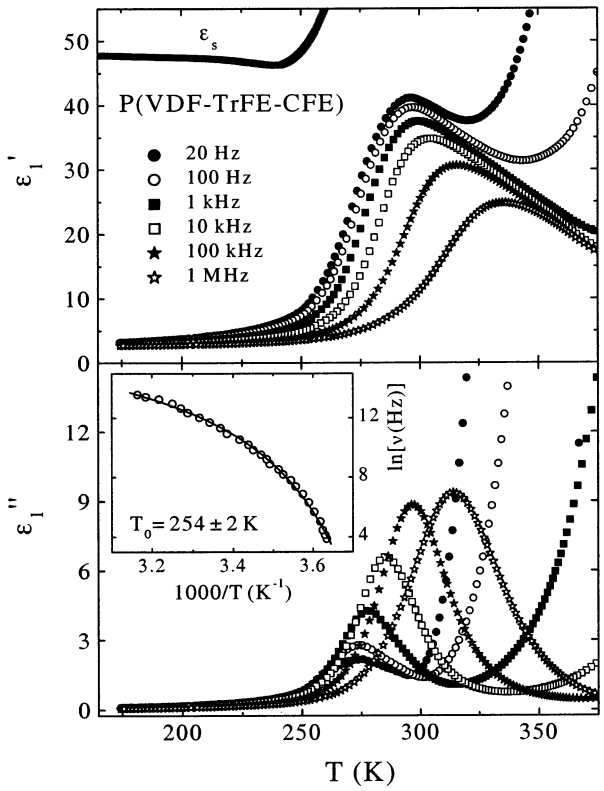

Figure 4. Temperature dependence of the real, ϵ_1', and imaginary, ϵ_1'', parts of the complex linear dielectric constant, measured at several different frequencies in the P(VDF−TrFE−CFE) terpolymer. The temperature dependence of the static dielectric constant ϵ_s, measured via charge accumulation technique, is also shown. The inset shows that the characteristic relaxation time follows the Vogel−Fulcher law.

210 K, dispersion in a_3 can be clearly seen. This explains why there is no anomaly in a_3 data at the glass transition temperature. Nonlinear dielectric data, obtained in PLZT−P(VDF−TrFE) composite, therefore reveal that the paraelectric-to-ferroelectric phase transition can be detected not only in linear but also in nonlinear dielectric response—notice a peak at T_c in the temperature dependence of ϵ_3—and in dielectric nonlinearity a_3.

B. Dielectric Properties of P(VDF−TrFE−CFE) Terpolymer. In this subsection the dielectric response of the P(VDF−TrFE−CFE) terpolymer is described. While a transition from the distorted trans−gauche paraelectric to all-trans ferroelectric phase occurs in the crystalline region of P(VDF−TrFE) copolymer and PLZT−P(VDF−TrFE) composite, addition of CFE converts all-trans chains in ferroelectric P(VDF−TrFE) copolymer into nanopolar regions, thus transforming the material into a relaxor ferroelectric system.

Figure 4 shows the temperature dependence of the real and imaginary parts of the complex linear dielectric constant, measured at several different frequencies in the P(VDF−TrFE−CFE) terpolymer. A broad dispersive dielectric maximum can be observed, which is a result of the fact that, as in dipolar glass and relaxor systems, ϵ_1' at a certain temperature which depends on the experimental time scale, i.e., frequency, starts to deviate from its static value. The temperature dependence of the static dielectric constant ϵ_s, measured via charge accumulation technique, could be due to the high electrical conductivity of this system determined only at temperatures below 240 K. Besides a broad dielectric maximum only the electrical conductivity contribution in ϵ_1' and ϵ_1'' can be observed, while there is no additional anomaly at $T_c \approx 343$ K, which means that addition of CFE completely transformed the ferroelectric material into a relaxor-like system. Also, the β-relaxation is in the dielectric spectra of P(VDF−TrFE−CFE) terpolymer overlapped by a relaxor-like dielectric dispersion. The inset to Figure 4 shows that the characteristic relaxation frequency, determined from peaks in $\epsilon_1''(T)$, follows the Vogel−Fulcher law $\nu = \nu_0 \exp[-U/k(T - T_0)]$ with the Vogel−Fulcher temperature $T_0 = 254 \pm 2$ K.

Figure 5 shows the temperature dependences of the third-order nonlinear dielectric constant ϵ_3 and dielectric nonlinearity a_3, measured at three different frequencies in the P(VDF−TrFE−CFE) terpolymer. The inset to Figure 5 shows that with a decreasing temperature a_3 undergoes a crossover from decreasing paraelectric-like to increasing glass-like temperature behavior. At a glance this dependence seems similar to the temperature dependence of a_3 in ferroelectric PLZT−P(VDF−TrFE) composite around T_c (inset to Figure 3). However, while a sharp anomaly occurs in the ferroelectric system exactly at T_c, here a smooth paraelectric-to-glass crossover takes place in the temperature region, where no phase transition occurs. In fact, such a crossover in a_3 is typical for relaxors: it has been detected in several relaxor systems[21,29,30] and is in accordance with the predictions of the spherical random-bond−random-field model of relaxor ferroelectrics.[21,31]

C. Temperature Evolution of the Relaxation Spectrum in Relaxor-like Electroactive Polymers. The complex linear dielectric constant data of P(VDF−TrFE−CFE) terpolymer, presented in Figure 4, are in

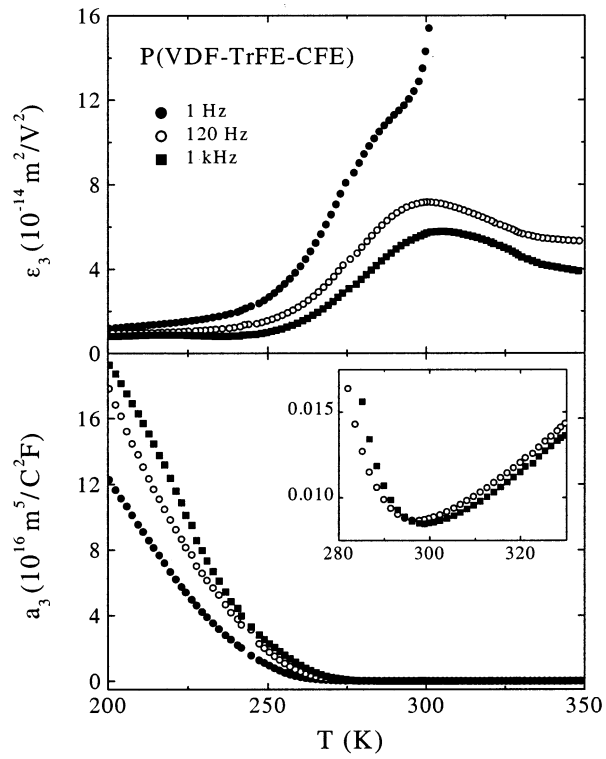

Figure 5. Temperature dependences of the third-order nonlinear dielectric constant ϵ_3 and dielectric nonlinearity a_3, measured at three different frequencies in the P(VDF−TrFE−CFE) terpolymer. The inset shows paraelectric-to-glass crossover in the temperature dependence of a_3.

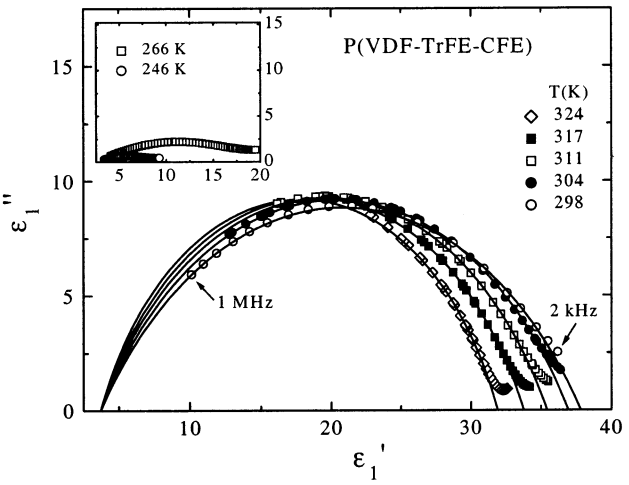

Figure 6. ϵ_1'' vs ϵ_1', measured at several different temperatures in the P(VDF−TrFE−CFE) terpolymer. Solid lines through the experimental data are fits to the Cole−Cole expression (eq 1). The inset shows that the relaxation spectrum becomes extremely polydispersive at lower temperatures.

Figure 6 shown in the ϵ_1'' vs ϵ_1' representation. One standard way to analyze these experimental data is fit to the Cole−Cole expression

$$\epsilon_1^* = \epsilon_\infty + \frac{\Delta\epsilon_1}{1 + (i\omega\tau)^{1-h}} \qquad (1)$$

where $\Delta\epsilon_1 = \epsilon_s - \epsilon_\infty$ is the dielectric relaxation strength, τ is the characteristic relaxation time, and h is the parameter describing the distribution of relaxation times. $h = 0$ describes monodispersive relaxation, while $0 < h < 1$ indicates a distribution of relaxation times in the system. This procedure can provide information about parameters ϵ_s, ϵ_∞, τ, and h. However, Cole−Cole plots cannot provide direct and independent information about the actual relaxation spectrum under investigation. Furthermore, since relaxation spectrum becomes extremely polydispersive with decreasing temperature, as can clearly be seen in the inset to Figure 6 (very flat ϵ_1'' vs ϵ_1' plots), this standard analysis can be performed only at higher temperatures.

On the other hand, the information on behavior of the relaxation spectrum and thus on dynamic processes can directly be extracted using the so-called temperature−frequency plot. This method has already been successfully applied to various glassy[32−34] and relaxor systems.[19,20] Its extended description is given in ref 32. The essential point is that by varying the reduced dielectric constant

$$\delta \equiv \frac{\epsilon_1'(\omega,T) - \epsilon_\infty}{\epsilon_s - \epsilon_\infty} = \int_{z_1}^{z_2} \frac{g(z)\,dz}{1 + (\omega/\omega_a)^2 \exp(2z)} \qquad (2)$$

between the values 1 and 0 different segments of the relaxation spectrum $g(z)$ are being probed ($\delta = 1$ probes the upper limit of the relaxation spectrum, i.e., the longest relaxation time). The distribution of relaxation times is limited by the lower and upper cutoffs z_1 and z_2.

Obviously, the knowledge of ϵ_s and ϵ_∞ is necessary for this procedure. Because of rapidly increasing polydispersivity with decreasing temperature, analysis of Cole−Cole plots, presented in Figure 6, provides values of ϵ_s only for temperatures above 290 K. On the other hand, it can be deduced from Figure 6 that ϵ_∞ is almost temperature independent, having a value of 3.8. The temperature dependence of the static dielectric constant ϵ_s, measured via the charge accumulation technique, could be due to the large electrical conductivity of this system at higher temperatures, determined only at temperatures below 240 K (see Figure 4).

Using obtained values of ϵ_s and the value of $\epsilon_\infty = 3.8$, the temperature−frequency plot was determined and is shown in Figure 7a. In practice, this procedure requires that within the set of the dielectric data at a given temperature T a frequency ν is found at which the prescribed value of δ is reached. Solid lines through the $\delta = 0.95$, ..., 0.70 data in Figure 7a are fits to the Vogel−Fulcher law, which demonstrate the diverging behavior of relaxation times. The inset to Figure 7a shows the dependence of the Vogel−Fulcher temperature T_0 on δ. Freezing temperature, where the longest relaxation time diverges, was determined as $T_f = T_0(\delta \rightarrow 1) = 269 \pm 2$ K. Its value is higher than the Vogel−Fulcher temperature $T_0 = 254$ K of the characteristic relaxation time (see inset to Figure 4) because the bulk of the relaxation times remains finite below T_f. The high-frequency part of the relaxation spectrum even remains active down to the lowest temperatures. Namely, the solid line through the $\delta = 0.01$ data in Figure 7a represents a fit to the Arrhenius law $\tau = \tau_0 \exp(E/kT)$. Since, because of high polydispersivity of the relaxation spectrum and large electrical conductivity, values of ϵ_s could not be measured in the temperature interval of 240−290 K, the temperature−frequency plot for terpolymer could not be determined for the values of $0.01 < \delta < 0.70$. However, results clearly indicate an asymmetric behavior of the relaxation spectrum of the P(VDF−TrFE−CFE) terpolymer: divergence of the

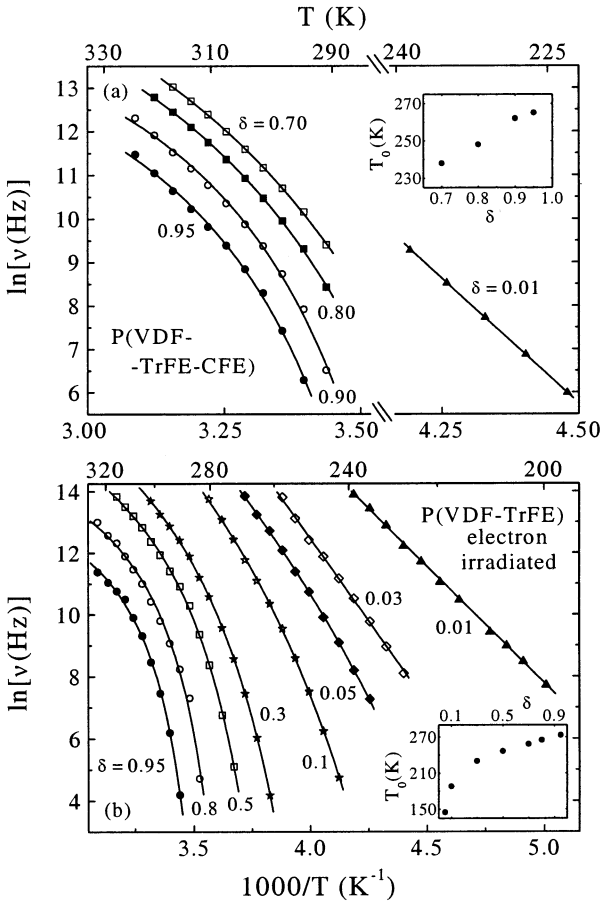

Figure 7. Temperature−frequency plot for several fixed values of the reduced dielectric constant δ in (a) the P(VDF−TrFE−CFE) terpolymer and (b) the electron-irradiated P(VDF−TrFE) copolymer. Solid lines are fits obtained with Vogel−Fulcher (δ = 0.95, 0.8, ..., 0.05) or Arrhenius (δ = 0.03, 0.01) expression. Because of high polydispersivity of the relaxation spectrum and large electrical conductivity, the temperature−frequency plot for terpolymer could not be determined in the range of $0.01 < \delta < 0.70$. Insets show the dependence of the Vogel−Fulcher temperature T_0 on δ in both relaxor-like systems.

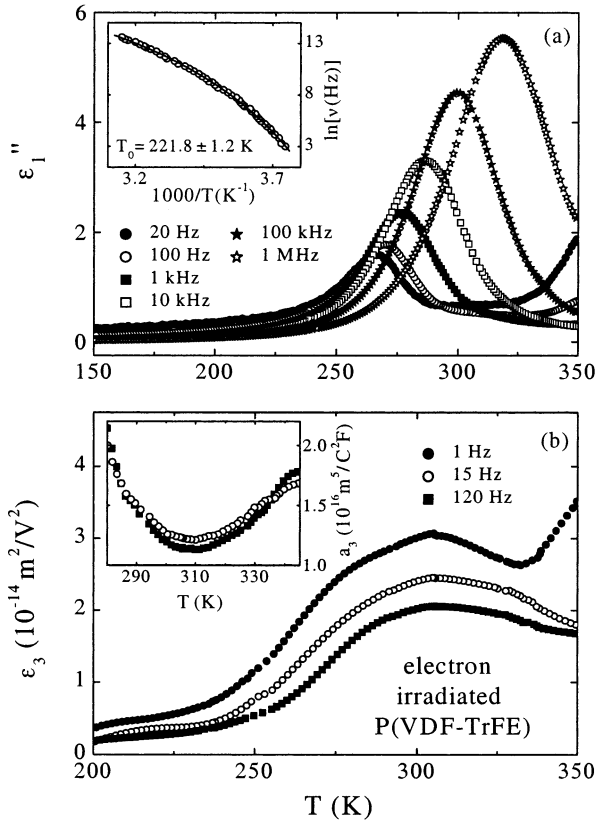

Figure 8. Relaxor-like dielectric response of the electron-irradiated P(VDF−TrFE) copolymer. (a) Temperature dependence of the imaginary, ϵ_1'', part of the complex linear dielectric constant, measured at several different frequencies. The inset shows that the characteristic relaxation time follows the Vogel−Fulcher law. (b) Temperature dependence of the third-order nonlinear dielectric constant ϵ_3, measured at three different frequencies. The inset shows paraelectric-to-glass crossover in the temperature dependence of the dielectric nonlinearity a_3.

longest relaxation time at a finite freezing temperature, while the shortest relaxation times remain active down to the lowest temperatures. Such an asymmetric behavior has already been detected in many glassy[25,32,33] and relaxor systems.[19,20]

Figure 7b shows the temperature−frequency plot in an electron-irradiated P(VDF−TrFE) copolymer. Here, because of smaller electrical conductivity as in P(VDF−TrFE−CFE) terpolymer, values of ϵ_s were measured in the whole temperature measurement range, and consequently the temperature−frequency plot was determined for values of the reduced dielectric constant δ in the whole range $0.01 < \delta < 0.95$. The asymmetric temperature evolution of the relaxation spectrum can clearly be seen. The freezing temperature, where the longest relaxation time diverges, was determined to be $T_f = 277 \pm 2$ K. The activation energy of 0.63 eV, resulting from the $\delta = 0.01$ data fit in electron-irradiated P(VDF−TrFE) copolymer, seems relatively high. However, as has already been reported,[18] activation energies for the irradiated copolymers are higher than that of the nonirradiated ones due to the random trans−gauche chain conformation (instead of the all-trans conformation) in the nonpolar phase, induced by irradiation process.

Figure 8 summarizes the most important dielectric properties of electron-irradiated P(VDF−TrFE) copolymer, which all show the relaxor-like properties of this system. As in the P(VDF−TrFE-CFE) terpolymer, a broad frequency dispersion in the linear and nonlinear dielectric constants, a Vogel−Fulcher temperature behavior of the characteristic relaxation time with a Vogel−Fulcher temperature $T_0 = 221.8 \pm 1.2$ K being considerably lower than T_f, and a paraelectric-to-glass crossover in the temperature dependence of the dielectric nonlinearity a_3 were observed. This demonstrates that the addition of the third bulky monomer in the P(VDF−TrFE) copolymer has the same effect on its properties as high-energy electron irradiation−transformation of the coherent polarization domain in normal ferroelectric P(VDF−TrFE) copolymer into nanopolar regions, thus transforming the material into a relaxor system. Therefore, both systems exhibit a giant electrostrictive response, which is a consequence of the expansion of the polar regions, whose lattice constant is significantly different than that of the nonpolar matrix, under the external electric field.

IV. Summary

Using linear and third-order nonlinear dielectric spectroscopy measurements, dynamic processes in vinylidene fluoride−trifluoroethylene-based electroactive polymers have been studied. It has been shown that

the addition of the PLZT ceramic powder into the P(VDF−TrFE) copolymer increases values of the real and imaginary parts of the complex dielectric constant, thus suggesting the possibility for tuning of dielectric properties of this piezoactive system by changing the PLZT/copolymer ratio. However, the dielectric response of the PLZT−P(VDF−TrFE) composite, demonstrating a transition from the distorted trans−gauche paraelectric to all-trans ferroelectric phase in the crystalline region and β-relaxation in the amorphous region of the system, is very similar to that of the P(VDF−TrFE) copolymer. This means that the dielectric relaxation processes of the copolymer matrix in fact determine the dielectric response of the composite.

On the other hand, high-energy electron irradiation or introduction of CFE drastically change the dielectric response of P(VDF−TrFE) copolymer. Both electron-irradiated P(VDF−TrFE) copolymer and P(VDF−TrFE−CFE) terpolymer show a dielectric response, typical for relaxor systems. A broad dispersion in linear and nonlinear dielectric constants and an extremely polydispersive relaxation spectrum at lower temperatures have been observed. The temperature−frequency plot analysis of the linear susceptibility revealed typical glassy (relaxor) asymmetric behavior of the relaxation spectrum: While the ergodicity of the system is effectively broken due to divergence of the longest relaxation time at a freezing temperature T_f ($T_f = 269 \pm 2$ K in terpolymer and $T_f = 277 \pm 2$ K in electron-irradiated copolymer), the bulk of the relaxation times remain active below T_f, the high-frequency part, obeying the Arrhenius law, even to the lowest temperatures. The temperature dependence of ϵ_s, reaching almost a constant value at lower temperatures, is by itself reminiscent of the dynamic behavior observed in various glassy systems. Also, the dielectric nonlinearity a_3 undergoes a crossover from decreasing paraelectric-like to increasing glass-like temperature behavior when approaching the freezing transition from above, which is another typical relaxor behavior. All these relaxor-like properties confirm that the addition of CFE and high-energy electron irradiation indeed transformed the coherent polarization domain in the normal ferroelectric P(VDF−TrFE) copolymer into nanopolar regions. A giant electrostrictive response, observed in both systems,[10,12] is therefore a consequence of the expansion and contraction of these polar regions, whose lattice constant is significantly different than that of the nonpolar matrix, under an external electric field.

Acknowledgment. This work was supported by the Ministry of Education, Science, and Sport of Slovenia and the Committee of Scientific Researches in Poland Grant No. 2P03B 121 24.

References and Notes

(1) Kawai, H. *Jpn. J. Appl. Phys.* **1969**, *8*, 975.
(2) Furukawa, T. *Phase Transitions* **1989**, *18*, 143.
(3) Tanaka, H.; Yukawa, H.; Nishi, T. *J. Chem. Phys.* **1989**, *90*, 6730. Tanaka, H.; Yukawa, H.; Nishi, T. *J. Chem. Phys.* **1989**, *90*, 6740.
(4) Furukawa, T. *Ferroelectrics* **1992**, *135*, 401.
(5) Tashiro, K. *Ferroelectric Polymers: Chemistry, Physics, and Applications*; Nalwa, H. S., Ed.; Marcel Dekker: New York, 1995.
(6) Ploss, B.; Ploss, B. *Polymer* **2000**, *41*, 6087.
(7) Hilczer, B.; Kulek, J.; Markiewicz, E.; Kosec, M. *Ferroelectrics*, in press.
(8) Odajima, A.; Takase, Y.; Ishibashi, T.; Yuasa, K. *Jpn. J. Appl. Phys.* **1985**, *24* (Suppl. 24-2), 881.
(9) Lovinger, A. J. *Macromolecules* **1984**, *18*, 910.
(10) Zhang, Q. M.; Bharti, V.; Zhao, X. *Science* **1998**, *280*, 2101.
(11) Xu, H.; Cheng, Z.-Y.; Olson, D.; Mai, T.; Zhang, Q. M. *Appl. Phys. Lett.* **2001**, *78*, 2360.
(12) Xia, F.; Cheng, Z.-Y.; Xu, H.; Li, H.; Zhang, Q. M.; Kavarnos, G. J.; Ting, R. Y.; Abdul-Sedat, G.; Belfield, K. D. *Adv. Mater.* **2002**, *14*, 1574.
(13) Viehland, D.; Jang, S. J.; Cross, L. E.; Wuttig, M. *Phys. Rev. B* **1992**, *46*, 8003.
(14) Sommer, R.; Yushin, N. K.; van der Klink, J. J. *Phys. Rev. B* **1993**, *48*, 13230.
(15) Cheng, Z.-Y.; Xu, T.-B.; Bharti, V.; Wang, S.; Zhang, Q. M. *Appl. Phys. Lett.* **1999**, *74*, 1901.
(16) Karaki, T.; Chou, I.; Cross, L. E. *Jpn. J. Appl. Phys.* **2000**, *39*, 5668.
(17) Bharti, V.; Xu, H. S.; Shanthi, G.; Zhang, Q. M. *J. Appl. Phys.* **2000**, *87*, 452.
(18) Bharti, V.; Zhang, Q. M. *Phys. Rev. B* **2001**, *63*, 184103.
(19) Levstik, A.; Kutnjak, Z.; Filipič, C.; Pirc, R. *Phys. Rev. B* **1998**, *57*, 11204.
(20) Kutnjak, Z.; Filipič, C.; Pirc, R.; Levstik, A.; Farhi, R.; El Marssi, M. *Phys. Rev. B* **1999**, *59*, 294.
(21) Bobnar, V.; Kutnjak, Z.; Pirc, R.; Blinc, R.; Levstik, A. *Phys. Rev. Lett.* **2000**, *84*, 5892.
(22) Kosec, M.; Kolar, D. *J. Phys., Colloq. C1* **1986**, *47*, C1379.
(23) Cheng, Z.-Y.; Olson, D.; Xu, H.; Xia, F.; Hundai, J. S.; Zhang, Q. M.; Bateman, F. B.; Kavarnos, G. J.; Ramotowski, T. *Macromolecules* **2002**, *35*, 664.
(24) Levstik, A.; Filipič, C.; Kutnjak, Z.; Levstik, I.; Pirc, R.; Tadić, B.; Blinc, R. *Phys. Rev. Lett.* **1991**, *66*, 2368.
(25) Menegotto, J.; Ibos, L.; Bernes, A.; Demont, P.; Lacabanne, C. *Ferroelectrics* **1999**, *228*, 1.
(26) Ogura, H.; Shimizu, T.; Motoyama, H.; Ochiai, M.; Chiba, A. *Jpn. J. Appl. Phys.* **1992**, *31*, 835.
(27) Stanley, H. E. *Introduction to Phase Transitions and Critical Phenomena*; Clarendon Press: Oxford, 1971.
(28) Fischer, K. H.; Hertz, J. A. *Spin Glasses*; Cambridge University Press: Cambridge, 1991.
(29) Glazounov, A. E.; Tagantsev, A. K. *Phys. Rev. Lett.* **2000**, *85*, 2192.
(30) Ko, J.-H.; Jiang, F.; Kojima, S.; Shaplygina, T. A.; Lushnikov, S. G. *J. Phys.: Condens. Matter* **2001**, *13*, 5449.
(31) Blinc, R.; Dolinšek, J.; Gregorovič, A.; Zalar, B.; Filipič, C.; Kutnjak, Z.; Levstik, A.; Pirc, R. *Phys. Rev. Lett.* **1999**, *83*, 424.
(32) Kutnjak, Z.; Filipič, C.; Levstik, A.; Pirc, R. *Phys. Rev. Lett.* **1993**, *70*, 4015.
(33) Hemberger, J.; Ries, H.; Loidl, A.; Böhmer, R. *Phys. Rev. Lett.* **1996**, *76*, 2330.
(34) De Sousa Meneses, D.; Simon, P.; Hauret, G.; Maglione, M. *Europhys. Lett.* **1996**, *36*, 461.

MA034149H